Sains Malaysiana 53(6)(2024): 1389-1403
http://doi.org/10.17576/jsm-2024-5306-13

Upcycling of Spent Copper Wires for Photocatalysis and Supercapacitor Applications

(Kitar semula Wayar Tembaga Dibelanjakan untuk Aplikasi Fotokatalisis dan Superkapasitor)

Cornelius Satria Yudha[1,*], Enni Apriliyani[2] & Meidiana Arinawati[3]

[1]*Chemical Engineering Department, Vocational School, Sebelas Maret University, Jl. Colonel Sutarto 150K Surakarta, Indonesia, 57126*
[2]*Center of Excellence for Electrical Energy Storage Technology, Sebelas Maret University, Jl. Slamet Riyadi 435 Surakarta, Indonesia, 57146*
[3]*Center of Excellence for Electrical Energy Storage Technology, Sebelas Maret University, Jl. Slamet Riyadi 435 Surakarta, Indonesia, 57146*

Received: 15 November 2023/Accepted: 29 April 2024

ABSTRACT

In this study, copper wires were upcycled as copper oxide (CuO) powder through hydrometallurgical and biotreatment processes, which are economically and environmentally attractive. Lactic acid, an organic weak acid, is chosen as the lixiviant to improve the sustainability of the leaching process; meanwhile, *Camellia sinensis* leaf extract is chosen for the biogenesis of CuO particles. The leaching behavior was investigated. A crystallized Cu powder was successfully generated during the biogenesis process, which became the precursor to CuO. The sintering of Cu resulted in high crystalline CuO particles with monoclinic structure (space group C2/c) based on several characterization methods such as X-ray diffraction analysis and Fourier transform Infrared spectroscopy. SEM images exhibited the submicron secondary particle with a raspberry-like shape of CuO and nanosized primary particles. The band gap of the as-prepared CuO is 3.17 eV. The as-prepared CuO particles were used as a photocatalyst and an active supercapacitor material. The photocatalytic performance was evaluated in a photodegradation process of acid orange 7 (AO7) and methyl orange (MO) dyes, which are considered harmful to the environment. The AO7 and MO photodegradation efficiency are 92.5 and 97.8, respectively. The electrochemical performance of CuO particles showed a pseudocapacitive behavior with a specific capacitance of 252 and 120 F/g at a current density of 0.5 and 5 A/g in 5 M of KOH electrolyte, respectively. This approach can be applied for numerous applications, specifically in overcoming heavy metal pollution from wide selections of metal-based wastes.

Keywords: Biogenesis; copper; leaching; photocatalyst; supercapacitor; waste

ABSTRAK

Dalam kajian ini, wayar kuprum dikitar semula sebagai serbuk kuprum oksida (CuO) melalui proses hidrometalurgi dan biorawatan yang lebih baik daripada segi ekonomi dan alam sekitar. Asid laktik adalah asid lemah organik, dipilih sebagai bahan pengikat untuk meningkatkan kemampanan proses larut lesap; Sementara itu, ekstrak daun *Camellia sinensis* dipilih untuk biogenesis zarah CuO. Tingkah laku larut lesap telah dikaji. Serbuk Cu terhablur berjaya dihasilkan semasa proses biogenesis yang menjadi pendahulu kepada CuO. Pensinteran Cu menghasilkan zarah CuO berhablur tinggi dengan struktur monoklin (kumpulan ruang C2/c) berdasarkan beberapa kaedah pencirian seperti analisis pembelauan sinar-X dan spektroskopi Inframerah transformasi Fourier. Imej SEM menunjukkan zarah sekunder submikron dengan bentuk seperti raspberi CuO dan zarah primer bersaiz nano. Jurang jalur bagi CuO seperti yang disediakan ialah 3.17 eV. Zarah CuO yang disediakan telah digunakan sebagai pemangkin foto dan bahan aktif untuk superkapasitor. Prestasi fotokatalitik telah dinilai dalam proses fotodegradasi pewarna jingga asid 7 (AO7) dan metil jingga (MO), yang dianggap berbahaya kepada alam sekitar. Kecekapan fotodegradasi AO7 dan MO masing-masing ialah 92.5 dan 97.8. Prestasi elektrokimia zarah CuO menunjukkan tingkah laku pseudokapasitif dengan kapasitans tertentu 252 dan 120 F/g masing-masing pada ketumpatan arus 0.5 dan 5 A/g dalam 5 M elektrolit KOH. Pendekatan ini boleh digunakan untuk pelbagai aplikasi, khususnya dalam mengatasi pencemaran logam berat daripada pelbagai pilihan sisa berasaskan logam.

Kata kunci: Biogenesis; fotomangkin; kuprum; larut lesap; superkapasitor; sisa

Introduction

Copper (Cu) wires have been widely used as the main component of electric cables for transportation, construction, internet networks, communication, and various electronic applications. A couple of decades ago, copper cables were effectively used to transmit data via electrical signals, allowing significant internet connection at a reasonable speed (Lambert et al. 2021). However, copper-based internet networking became less efficient due to performance instability during data transmission, resulting in low data transfer, signal strength, and financial losses in business sectors. With the invention of reliable, superior, and resilient fiber optics, the use of copper wires was reduced drastically. As a result, spent copper wires are generated in large amounts (Addanki, Amiri & Yupapin 2018). Usually, this type of cable can be recycled for reuse; however, most wires were processed using the high-energy pyrometallurgical technique. Physical processing of copper wires was conducted at a lower temperature, such as dismantling, shredding, and separation using gravity or electromagnets. These approaches generate residual copper, often left unprocessed but still economically valuable.

The hydrometallurgical approach has significant advantages compared to the physical and pyrometallurgical techniques. Hydrometallurgical processing requires a relatively low temperature at atmospheric pressure, which is beneficial for large-scale implementation. Specifically, the leaching process often has high leaching efficiency, especially using cheap and commercially available mineral acids such as nitric acid (HNO_3), sulfuric acid (H_2SO_4), and hydrochloric acid (HCl) (Soraya Ulfa et al. 2019). Bioleaching (biohydrometallurgy) has similar features, with lower metal recoverability and lower leaching efficiency and significantly longer processing time (Lambert et al. 2021). Therefore, acid-leaching using acids is still economically feasible for Cu recovery. To enhance the eco-friendliness of the process, researchers have performed leaching using organic acids. Organic acids are considered weak, resulting in a safer approach and handling than mineral acids. In the past years, organic acids have been utilized to extract copper from ores, rocks, and various electronic waste (Li et al. 2012; Zhuang et al. 2019). Acetic acid, citric acid, oxalic acid, and maleic acid have been employed as a lixiviant for the Cu recovery of various materials (Lisińska et al. 2022; Nagarajan & Panchatcharam 2023). The use of lactic acid, widely used in food, cosmetics, and medicine, as a lixiviant is also promising; however, it was scarcely and seldom reported.

The recovered Cu-containing solution is potentially adapted as advanced materials for Li-ion batteries, sensors, and photocatalysts (Bekru et al. 2022; Seong & Manthiram 2020; Shah et al. 2019). The solution route method for Cu-based advanced materials has been extensively investigated, including chemical precipitation, pechini's method, spray pyrolysis, and electrochemical method, with outstanding study results. The as-prepared copper-based material has antifungal, antibacterial, and anticancer activity, making it suitable for medicinal application (Devanthiran et al. 2021). Nowadays, a greener and more cost-effective method is preferred due to environmental and economic perspectives responsible for the technology's sustainability. Biogenesis of copper-based materials is an interesting topic and has also been successfully conducted to produce material with exceptional characteristics by utilizing plant extracts (Cuong et al. 2022; Dharshini et al. 2023). Therefore, lactic acid-assisted leaching and biogenesis are interesting combinations that can be used to upcycle spent copper wires to Cu-based material.

Copper-based materials, such as Cu or CuO nanoparticles, have been successfully fabricated through metal reduction and capping mechanisms using leaf extracts of various plants such as soursops, kales, beets, olives, and palms (Devanthiran et al. 2021; Muhammad et al. 2021; Shanmugam et al. 2018). Even though many other plant parts can be utilized as the capping agent, leaves are often preferred due to their abundance, cost, and biomolecule content which helps the formation of materials and the sustainability of the technology. A tea leaf (*Camellia sinensis)* is a promising candidate for the biogenesis of Cu/CuO materials due to its high number of tannins, flavonoids, and polyphenol content (Emima Jeronsia et al. 2019). Tea is also a cheap and traditional beverage in many countries, and it is rated as the most consumable drink, besides water.

This study will explore the leaching process of copper wire using lactic acid as the lixiviant. Also, the recovered copper ions were used along with black tea extract to form Cu/CuO advanced material biogenetically. The as-produced Cu/CuO materials will be used for the supercapacitor active material and photocatalysts to photodegrade dye pollutants, namely acid orange 7 (AO7) and methyl orange (MO). The overall process is environmentally and economically attractive, considering the rapidly growing energy sector technology and environmental issue of genotoxic organic pollutants.

Materials and Methods

Materials

The black tea (*Camellia sinensis*) leaf was obtained from an Indonesian tea producer (PT Teh Kartini Nasional, Indonesia). The copper cable was obtained during the alteration of copper cable to fiber optics. Lactic acid (Merck, Germany) was used as the lixiviant. NaOH (Merck, Germany) was used as a pH controller.

Methods

Extraction of dry Camellia sinensis leaves 25 grams of pre-dried and pre-ground tea leaves were added to 500 mL of boiling water in a 1 L beaker glass. The beaker glass was covered, and the maceration lasts for 30 min. The beaker was cooled to room temperature, and the tea residue was separated using a vacuum filter. The volume of the tea extract was adjusted to 500 mL using deionized water.

Copper cable leaching using lactic acid The copper wire was protected with rubber and plastic. The rubber and plastic were peeled off. The as-obtained copper wire was cut into 0.5 cm lengths, washed, dried in an oven, and stored in a dry container. The cable was leached using 1 M lactic acid. The solid-to-liquid (S/L) ratio was maintained at 25:1000. 5%v/v of H_2O_2 was added to the solution as an oxidizing agent. The leaching was conducted for 5 hours at 70 ℃ to obtain a green-blue copper (II) lactate solution. The solution was analyzed using AAS and UV-visible to predict the leaching behavior of spent copper cable.

Biogenesis of Cu powder 50 mL of as obtained copper (II) lactate solution was mixed with 950 mL of *Camellia sinensis* extract. The mixture was continuously stirred at 300 rpm. After 30 min, the 4 M NaOH solution was added dropwise to the mixture to achieve a pH of 10-11. After the desired pH was achieved, the mixture was allowed to age for a total of 24 h. Afterward, a red-brownish suspension was centrifuged. The supernatant was carefully removed and replaced with deionized water until the pH solution was neutral. The formed precipitate was recovered, dried in the oven, and labeled as Cu-CS.

Formation of CuO powder The as-prepared powder was dispersed in a NaOH-containing solution with a pH level of ~10. The suspension was heated at 80 °C to achieve a black precipitate. The precipitate was taken using the same technique for Cu powder recovery. The as-prepared powder was labeled CuO-CS-LT. The CuO-CS-HT was obtained by annealing of Cu-CS at 500 °C for 3 h under an air atmosphere.

Material characterization The morphological and quantitative analysis was performed using a scanning electron microscope (SEM) by FEI Inspect-S50, FEI Company, USA, at 20 kV. The X-ray diffraction pattern of the samples was analyzed using D2-Phaser Bruker, Germany. The FTIR analysis was conducted using IR-Spirit, Shimadzu, Japan. TG/DTA analysis was performed using Thermogravimetric Analyzers 60, Shimadzu, Japan. UV-Visible spectra of the CuO powder were analyzed using Specord 200 Plus, Analytik Jena, Germany.

Electrochemical Performance Analysis in a Supercapacitor The as-prepared CuO-CS was mixed with Acetylene black (AB) and Polyvinyl difluoride (PVDF) at a gravimetric ratio of 80:10:10. The mixture was dispersed in N-methyl 2 pyrrolidone (NMP) solvent to obtain a stable and homogenized slurry. The slurry was coated on a stainless-steel plate with a 10 mg/cm^2 mass loading. The coated plate was dried in a vacuum oven to obtain CuO electrodes. The electrode was tested using a three-electrode system. 5 M KOH (Merck, Germany) was used as the electrolyte. Ag/AgCl and Pt wire were used as the reference and counter electrodes. The cyclic voltammetry was conducted at various scan rates. Galvanostatic charge discharge was also conducted using various current densities. Both cyclic voltammetry and GCD analysis were performed using EZ-Ware, NuVant Potentiostat, USA.

Photocatalytic activity of CuO-CS The photocatalytic activity of the as-prepared CuO was evaluated by photodegradation analysis of AO7 and MO dye. 500 mL of 20 ppm of each dye was prepared as a pollutant sample. 50 mg of CuO sample was added to each solution. As a control, solutions with no CuO were also prepared. The CuO was allowed to be dispersed for 30 min to ensure chemical equilibrium in the photocatalyst. H_2O_2 (Merck, Germany) was added to the solution with a final concentration of 10 mM. The dispersion was put under UV light. The UV-Visible spectra of the solutions were collected at various times.

Results and Discussion

Leaching behavior of copper cable in lactic acid and characterization of the leachate

Leaching behavior analysis The results of the analysis of the UV-Vis spectra show that the samples shown in Figure 1(a) contain CuO-LA samples with a comparison of samples with and without the addition of H_2O_2. The copper can be leached due to the presence of oxidized state of copper which is thermodynamically feasible to be leached using acid. The addition of H_2O_2 in this experiment aims to increase the leaching efficiency of the samples. The results of the UV-Vis spectral analysis, the addition of H_2O_2 was very crucial on the leaching efficiency marked by the high peak at a wavelength of 802 nm. Based on the FTIR spectra in Figure 1(b), the Copper (II) lactate extract has the molecular formula $Cu(CH_3CHOHCOO)_2$. The reactions that occur in the leaching process are as follows:

$$CuO(s) + {}_2CH_3CHOHCOOH \rightarrow Cu(CH_3CHOHCOO)_2 + H_2O(g) \quad (1)$$

Figure 2(a) shows the behavior of copper cable leaching with lactic acid. It can be seen that the concentration of the solution always increases with increasing time. The rate of reaction become slower as the efficiency approach 90%. From the results of comparing AAS data with UV-Vis, there is no significant difference in the measurement results, this indicates that UV-Vis spectroscopy can be used to evaluate the leaching behavior of copper in various acids for future project (Habbache et al. 2009). Based on the leaching data, we performed a preliminary kinetic study to predict the suitable reaction mechanism. Shrinking Core Model (SCM) is often used to predict the kinetic model of heterogenous reaction. However, the particle is often considered as a spherical and non-porous, which will affect the leaching mechanism prediction. The overall reaction is often controlled by the internal reaction or external physical driving force such as mass transfer. The dissolution kinetic of copper can be expressed in these equations:

For mass transfer in the liquid, the equation is:

$$LE = k \times t \quad (2)$$

For surface reaction control, the equation is:

$$1 - (1 - LE)^{\frac{1}{3}} = k \times t \quad (3)$$

For diffusion of product layer, the equation is:

$$1 - \frac{2}{3}LE - (LE)^{\frac{2}{3}} = k \times t \quad (4)$$

where LE is leaching efficiency. The kinetic plot according to these equation can be seen in Figure 2(b)-2(d). Based on the plots and the R^2 values, the reaction is controlled by surface reaction which is consisten to

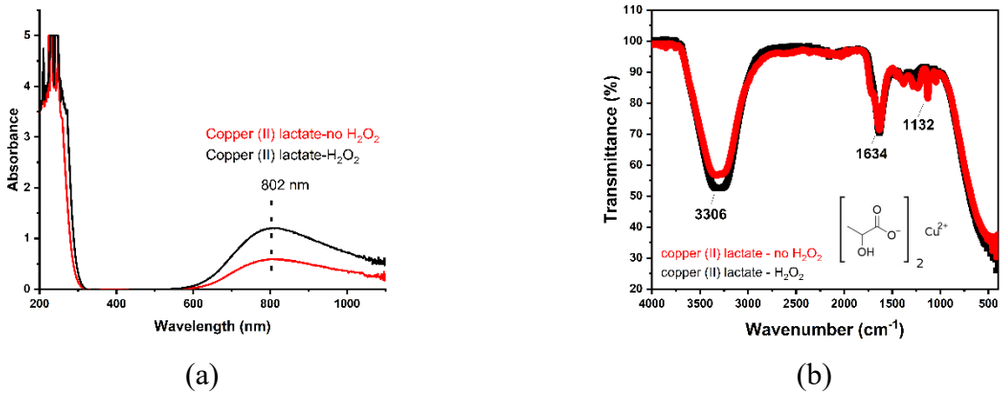

(a) (b)

FIGURE 1. (a) UV-visible spectra and (b) FTIR spectra of copper extract (copper lactate) by leaching process for 120 min with (black) or without the addition of 5% v/v H_2O_2 (red)

previous studies (Habbache et al. 2009; Li et al. 2018, 2012). The surface reaction is relatively slow due to the utilization of organic weak acid such as lactic acid, which require more than 5 h to achieve full copper dissolution.

XRD analysis The extract obtained was used to produce Cu particles by the biogenesis method. Figure 3(a) shows the results of the XRD analysis of Cu, CuO samples formed at low temperature (80 °C) (CuO-CS-LT) and CuO formed at high temperature (500 °C) (CuO-CS-HT). It can be seen that pure copper particles can be seen in the X-ray diffraction pattern of Cu-CS sample which in accordance to JCPDS 003-1018 proving that face-centered cubic (FCC) structured copper can be formed from the biogenesis process with black tea extract. The CuO-CS-LT sample was formed when Cu is oxidized under alkaline conditions at a mild temperature (80 °C). Meanwhile, based on the diffraction pattern, CuO-CS-LT showed Cu_2O phase according to JCPDS 05-0667 and CuO phase according to JCPDS 45-0937 are accompanied by sodium impurities which indicate that the oxidation is not uniform or partial oxidation was occurred. The crystallinity of Cu-CS is reduced during the low-temperature oxidation due to the peaks broadening and intensity reduction in the diffraction pattern. This phenomenon occurs due to the leaching

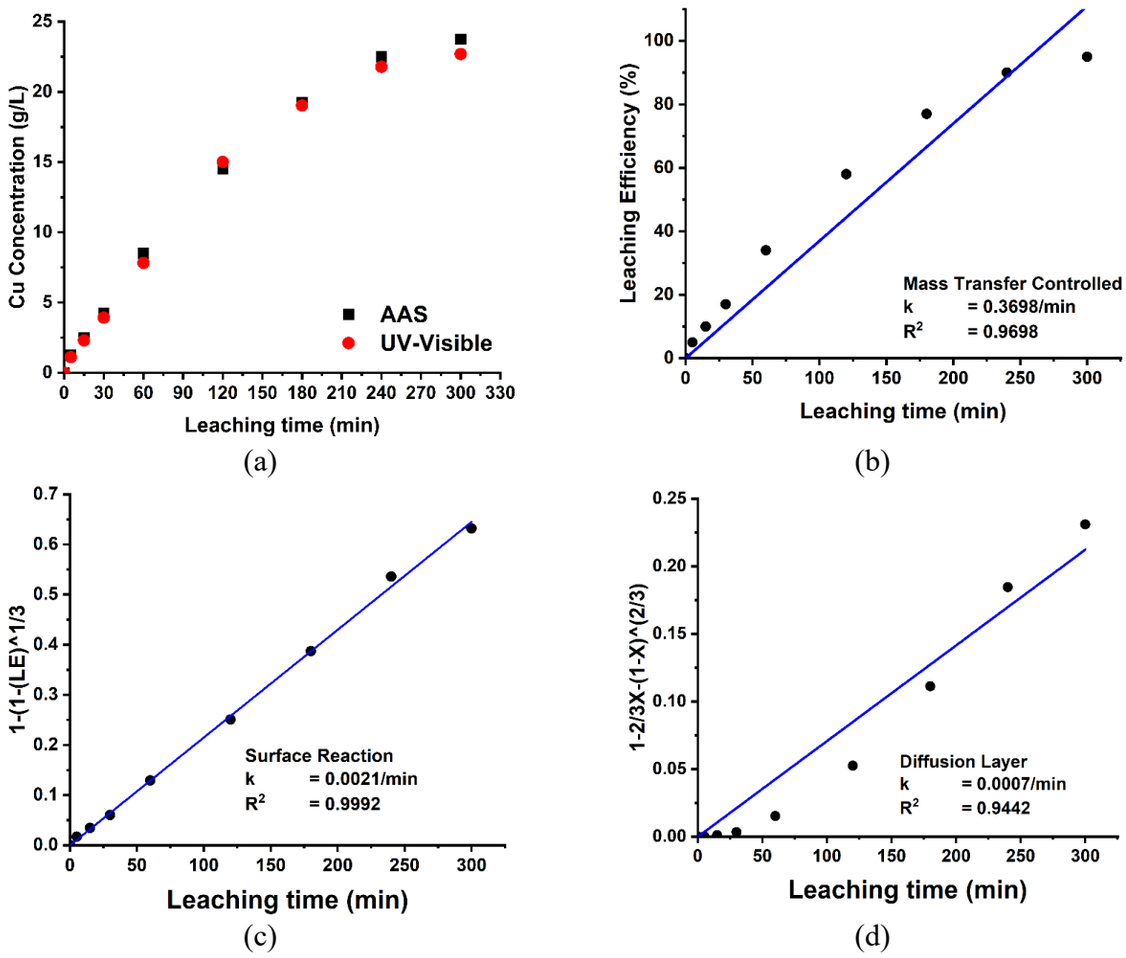

FIGURE 2. Leaching behavior of spent copper cables using 1 M lactic acid and 5%v/v H_2O as lixiviant at S/L of 25/1000 and the preliminary copper leaching kinetic study using shrinking core model : (b) Mass Transfer Controlled ; (c) Surface reaction controlled; (d) Diffusion layer controlled

of the as-prepared Cu-CS resulting in poor crystalline property of CuO-CS-LT (Gennero De Chialvo, Marchiano & Arvía 1984). A pure CuO phase is formed which is characterized by the formation of a crystalline phase that corresponds to the miller index reference (Dana & Sheibani 2021). Based on structural analysis, CuO-CS-LT has a monoclinic crystal structure with space group C_2/c and lattice parameters a, b, c, α, β, and γ, respectively, 4.703, 3.457, 5.123, 90, 90 and 93.825°. This is in accordance with other studies that have been performed. Based on calculation using debye-scherer' equation, the CuO-CS-LT sample has a crystallite size of 12.96 nm (Hyba et al. 2023; Liu et al. 2020). Based on the XRD data, high-temperature sintering is preferred in order to obtain high purity CuO-NPs.

FTIR analysis Figure 3(b) shows the FTIR spectra of Cu-CS samples derived from pure copper and CuO-CS-HT samples obtained from heating Cu particles. In

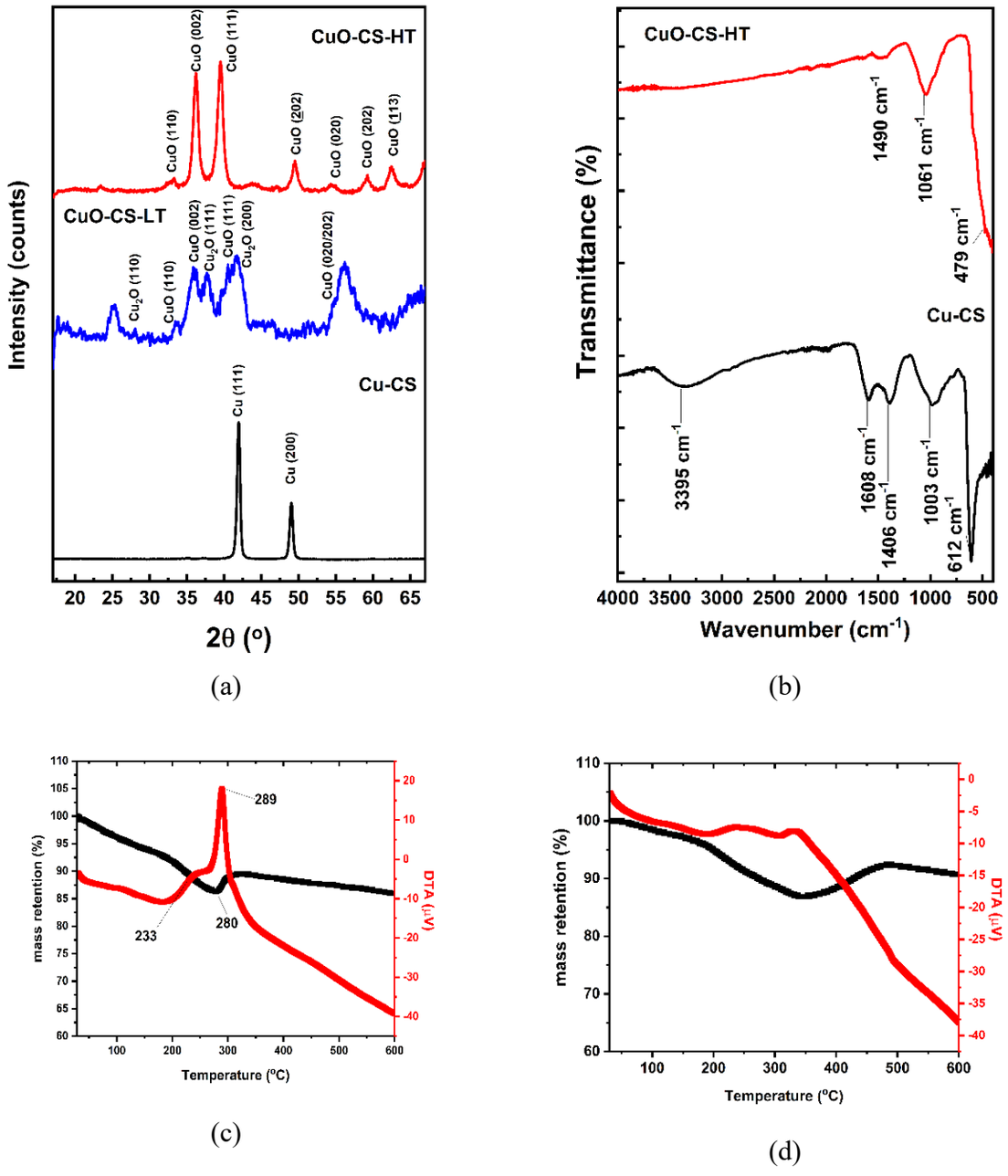

FIGURE 3. (a) X-ray diffractograms of Cu-CS, CuO-CS-LT, and CuO-CS-HT; (b) FTIR spectra of samples Cu-CS and CuO-CS-HT; and, TG/DTA curve of Cu-CS samples under (c) air and (d) N_2 atmosphere

the Cu-CS sample, it can be seen that there are several significant peaks that appear, such as at wave numbers 3395/cm and 1608/cm which indicate the presence of OH groups caused by adsorbed water molecules. The peak that appears at 1460/cm is indicated as the C=O group and at 1003/cm it is indicated as an asymmetric C-O group. There is a sharp peak that appears at 612/cm which is indicated as CuO. In Figure 3(b) it can be seen that the CuO-CS-HT sample has a significant peak that appears at wavenumber 1490/cm which is indicated as an OH group due to the adsorption of water molecules in the sample. There is a sharp peak observed at 1061/cm which indicates the presence of a C-O group. The appearance of the C-O group can come from the adsorption of carbon dioxide from moist air. Moreover, the presence of CuO or metal oxide bonds is indicated by the formation of peaks in the range of 500-450/cm (Saquf et al. 2018; Varughese, Kaur & Singh 2020).

TG/DTA analysis. TG/DTA analysis of Cu samples under conditions of airflow and N_2 gas flow can be seen in Figure 3(c) and Figure 3(d), respectively. In Figure 3(c), it can be concluded that Cu-CS can be thermally oxidized under air at a temperature of about 280 °C which is indicated by a significant increase in mass, the TG curve shows a decrease of mass up to 280 °C; afterwards, the TG curve was increased significantly along with an occurrence of two exothermic peaks at 233 °C and 289 °C. This phenomenon can be direct evidence of several processes: (i) The elimination of water molecules, which is indicated by the decreasing of TG and DTA curves; (ii) the decomposition of organic residues; and (iii) the oxidation of copper, indicated by a sharp exothermic peak at 289 °C and increasing of TG curve. After the oxidation occurs, it can be seen that both TG and DTA curves are declining gradually, which indicates a continuous removal of volatile matters in the Cu-CS samples. The exothermic peaks cannot be found in the TG/DTA curve of Figure 3(d) due to the absence of oxygen or inert conditions, which prevents the oxidation of Cu but allows organic substances to decompose due to endothermic pyrolysis. The results of the TG/DTA study prove that the sintering process is necessary to remove organic residue from the biogenesis process, thus obtaining a pure CuO. The overall reaction during the heat treatment under air can be seen in the Equations (5) and (6); meanwhile the predicted reaction during the heat treatment in an inert atmosphere can be seen in Equation (7) (Jadhav et al. 2011; Tanna et al. 2016).

$$Cu_{(s)} + ½\ O_2 \rightarrow CuO_{(s)} + \text{heat} \quad (5)$$

$$C_xH_yO_z\ (\text{residue})_{(s)} + (z/2+y/4)\ O_2 \rightarrow xCO_{2(g)} + y/2H_2O_{(g)} + \text{heat} \quad (6)$$

$$C_xH_yO_x(\text{residue})_{(s)} + \text{heat} \rightarrow C_{(s)} + CO_{(g)} + H_{2(g)} \quad (7)$$

SEM-EDX-Mapping analysis The results of the morphological analysis of Cu-CS and CuO-CS-HT samples can be seen in Figure 4(a) and 4(b) Cu-CS samples and 4(c), 4(d) CuO-CS-HT samples which were showing submicron secondary particles with quasi-spherical and raspberry-like surface and nano-sized primary particles. Although, in the synthesis of CuO samples, heating is carried out but does not affect the shape of the sample significantly, the shape of the CuO sample particles that are formed is uniform and looks denser with rough surface texture. In addition, the distribution of particles in the samples is relatively narrow. The average secondary particle size of these two samples was ~400 nm, while the primary particle size was in the range of 20-90 nm (Dubal et al. 2013; Liu et al. 2020).

To ensure the results of the SEM-EDX analysis, this study also tested the atomic mapping analysis (mapping). Atomic mapping analysis results (mapping) Cu-CS and CuO-CS-HT can be seen in the inset of Figure 4(a) Cu-CS sample and (c) CuO-CS-HT sample. In the image of the results of the Cu-CS sample atomic mapping test (inset Figure 4(a), 4(c)) it can be seen that the distribution of Cu in the sample is more dominant while the distribution of oxygen in the sample is not dominant, this proves that the Cu-CS biogenesis process was carried out successfully. Meanwhile, the results of the analysis of atomic mapping (mapping) of CuO-CS-HT samples can be seen that Cu and Oxygen have a consistent distribution according to their location, this is consistent with the results of the XRD analysis in Figure 3(a).

The results of the EDX analysis of Cu and CuO samples showed that both samples contained several elements such as Cu, O, C, Si, and Ca with the %atom ratio shown in Table 1. In the EDX test results of Cu samples, the elements O (oxygen), C (Carbon), Si (Silica) and Ca (Calcium) appeared, this was due to the presence of residues *Camellia sinensis* which cannot be simply washed away. Whereas in the CuO sample the elements O (oxygen) appear due to the oxidation of Cu at high temperatures, besides that there are also elements Si, Ca in the CuO sample due to the presence of residues *Camellia sinensis* which cannot be removed during the sintering process, however, the amount of Si and Ca is very low (less than 0.6%). High amount of carbon is associated by the background carbon tape of the sample during the analysis.

TABLE 1. Quantitative analysis of samples with EDX

Elements	%Cu atom (%)	%atom CuO (%)
Cu	21	13
O	32	27
C	46	59
Si	0.6	0.5
Ca	0.4	0.5

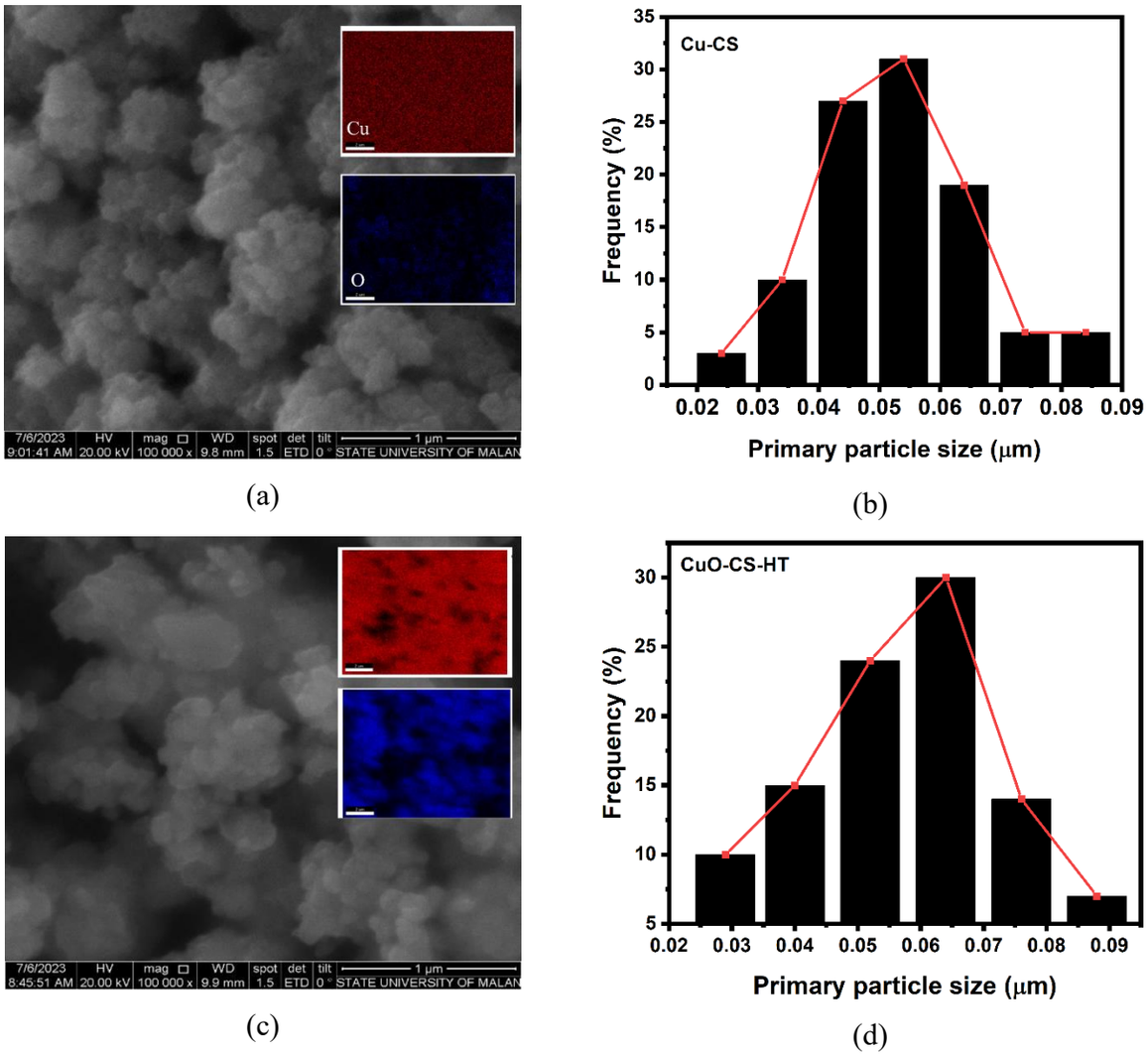

FIGURE 4. SEM-EDX mapping images (a,c) and particle size histogram (b,d) of Cu-CS (top) and (c,d) CuO-CS-HT (bottom) samples

UV-Vis Diffuse Reflectance Spectra Analysis DRS UV-Vis analysis was carried out to determine the semiconductor properties of CuO through calculations band gap on the Tauc plot. The UV-Visible Spectra and the Tauc Plot can be seen in Figure 5(a) and 5(b). Energy Band-gap can be calculated from the absorption spectra. In the UV-VIS absorption spectrum of the CuO-CS-HT sample it only shows one maximum peak which is shown in the range of about 345 nm which is the characteristic band gap of CuO. In several literatures describing the synthesis of CuO nanoparticles with various techniques will generally produce a mixture of CuO and Cu_2O. In this experiment, results were obtained indicating the formation of the CuO phase. Based on the calculation, the energy value band-gap sample is 3.17 eV which is in the range of semiconductor materials. The band gap results obtained are higher than the literature CuO values of 1.8-2.5 eV. This could be due to the effect of the sample quantum size (Saquf et al. 2018).

Photocatalytic Degradation of Organic Pollutant (Acid Orange 7 and Methyl Orange) The photocatalytic activity of CuO-CS-HT tested against degradation with Acid Orange 7 (AO7) and Methyl Orange (MO) using UV light is shown in Figure 5. The UV-VIS absorbance in Acid Orange 7 sample showed the highest peak at 492 nm (Figure 5(c)). Meanwhile, the UV-VIS absorbance in the Methyl Orange (MO) sample showed the highest peak at 460 nm (Figure 5(e)). In the experiment, Acid Orange 7 and Methyl orange samples were carried out for 1 h, where the longer the irradiation time using UV light, the absorbance of the samples decreased. Degradation using Acid Orange 7 for 1 h experienced a decrease in absorbance of 92.5% as shown in Figure 5(d) and degradation using Methyl Orange for 1 h experienced a decrease in absorbance of 97.8% (Figure 5(f)). In general, the processes involved in photocatalysis include absorption of light, generation and dissolution of e−/h+ pairs, transfer of e−/h+ to active reactions for redox reactions, e−/h+ recombination, and adsorption/desorption of reactants/products forming radical species which oxidize organic pollutants. With the addition of small amount of H_2O_2, the material behave like a photo-Fenton catalyst (Betim et al. 2023; Dong, Xing & Zhang 2020). We also compare the result of the study without CuO-NP photo-Fenton catalyst with MO and AO7 degradation efficiency of 23.7% and 33.2%, respectively, irradiated at the same time. Acid Orange 7 and Methyl Orange compounds have a high tendency to be oxidized into simple compound such as CO_2, H_2O, and carboxylic acids (Bekru et al. 2022; Widiyandari et al. 2023), with an addition of H_2O_2, the hydroxyl radical increases and the degradation occurred rapidly. Table 2 compares the photodegradation performance of the current study to the previous studies using similar CuO synthesis method. Based on Table 2, CuO NPs was successfully synthesized using various biomass, part of biomass, and copper precursor. The result of our study is comparable with the other researches (Qaderi, Mamat & Abdul Jalil 2021; Raub et al. 2022). The use of copper-based waste can improve the sustainability of the product, thus, this study can provide a new perspective on finding the copper sources. To improve the value of the as-prepared CuO-CS-HT, the sample was used as an active material for aqueous supercapacitor. The same approach was used by Nwanya et al. (2019) by utilizing corn husk extract as the capping agent for CuO synthesis and applied it as an asymmetrical supercapacitor.

Electrochemical Performance of CuO-CS-HT Figure 6(a) displays the cyclic voltammetry curve of CuO-CS-HT electrode at scan rates of 2, 5, 10, 20, 30, 50, 80, and 100 mV/s performed using three-electrode system as presented in Figure 6(b). The area inside the curve increased with the increasing of scan rate as a result of capacitive behavior of CuO-CS-HT electrode. Based on the curve's shape, the CuO-CS-HT in 5 M KOH electrolyte has a pseudocapacitive behavior. This is consistent with previous researches that transitional metal is considered as pseudo-capacitor whereas during the electrochemical process ions of the electrolyte were electrochemically stored on the surface of the CuO. Figure 6(c) presents the galvanostatic charge discharge of CuO-CS-HT in three electrode system. The specific capacitance of CuO-CS-HT at current density of 0.5, 1, 2, 5, and 10 A/g is 252, 192, 168, 120, and 50 F/g, respectively. The Ragone plot can be seen in Figure 6(d), which proved that CuO-CS-HT is suitable to be used as supercapacitor due to its power density range of 100-10.000 W/kg (Dubal et al. 2013; Nisha, Vidyalakshmi & Sirajunnisa 2020). Table 3 compares the electrical performance of CuO prepared using various techniques which also showed that the as-prepared CuO has comparable electrochemical performance with the previous studies.

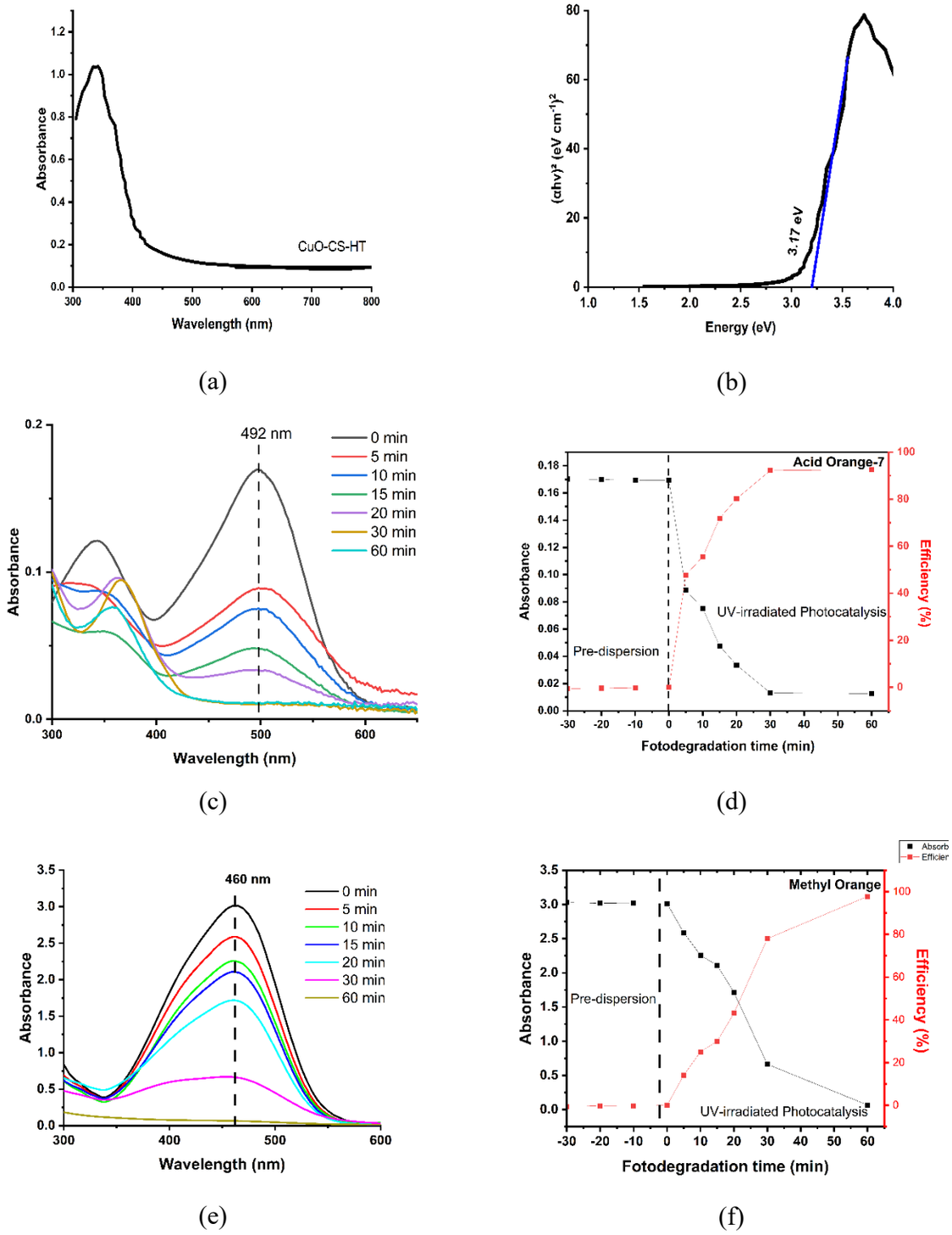

FIGURE 5. (a) UV-Vis DRS spectra; (b) Tauc plot, and the photocatalytic performance of CuO-CS-HT in photodegradation of (c,d) Acid Orange 7 (AO7) and (e,f) Methyl Orange (MO) using UV-visible spectroscopy

TABLE 2. Comparison of the biotreated CuO photocatalytic performances

Biomass	Part	Cu Precursor	Morphology	Size (nm)	Dye	Source	Presence	Efficiency (%)	Time	Band Gap (eV)	Ref.
Triticum aestivum (T. aestivum)	seeds	$CuSO_4.5H_2O$	hexagonal, cylindrical	20.76	4-Nitrophenol (4-NP)	UV Light	$NaBH_4$	97.6	5 day	4.13	Rostami-Vartooni (2017)
Stachys Lavandulifolia	flower	$CuSO_4.5H_2O$	Spherical	20–35	Crystal Violet (CV)	UV Light	H_2O_2	97	5 h	3.87	Hojat et al. (2021)
Rumex crispus	seeds	$CuCl_2 \cdot 2H_2O$	Spherical	8-60	4-Nitrophenol (4-NP) Congo Red (CR)	UV Light	$NaBH_4$	>90	5 min	-	Rostami-Vartooni (2017)
Aglaia elaeagnoidea	flower	$Cu(NO_3)_2.3H_2O$	Spherical	36–54	Congo Red	-	$NaBH_4$	90	<1 min	-	Manjari et al. (2017)
Annona muricata	leaf	$CuSO_4.5H_2O$	spherical	30-40	Reactive Red Methyl Orange	Visible Light	-	90	60 min	-	Kayalvizhi et al. (2020)
Euphorbia maculata	leaf	$CuSO_4.5H_2O$	Spherical	18	Congo Red Methylene blue (MB) Rhodamine B (RhB)	UV Light	-	96 85 89	60 min	-	Pakzad, Alinezhad & Nasrollahzadeh (2019)
Pterolobium hexapetalum	leaf	$CuSO_4.5H_2O$	spherical	10-50	Reactive Black (RB)	UV Light	-	98	120 min	-	Nagaraj et al. (2019)
Punica granatum	peels	$CuCl_2 \cdot 2H_2O$	spherical	10-5	Methyl Orange (MO)	UV Light	-	65	90 min	1.4 – 2.3	Ghidan, Al-Antary & Awwad (2016)
Rauvolfia serpentina	leaf	$Cu(NO_3)_2.3H_2O$	Sponge Like	10-20	Trypan Blue (TB)	UV Light		95	160 min	-	Lingaraju et al. (2015)
Scoparia dulsis	leaf	$Cu(NO_3)_2.3H_2O$	Spherical	12-16.6	Methylene blue Methyl orange	UV Light	-	97.3 94.4	180 min	3.96	Meghana Navada et al. (2020)
Camellia sinensis	leaf	Spent cable (waste) /$Cu(CH_3COHCOO)_2$	Raspberry-like	20-90	Acid Orange 7 Methyl Orange	UV Light	H_2O_2	92.5 97.8	60 min	3.17	This study

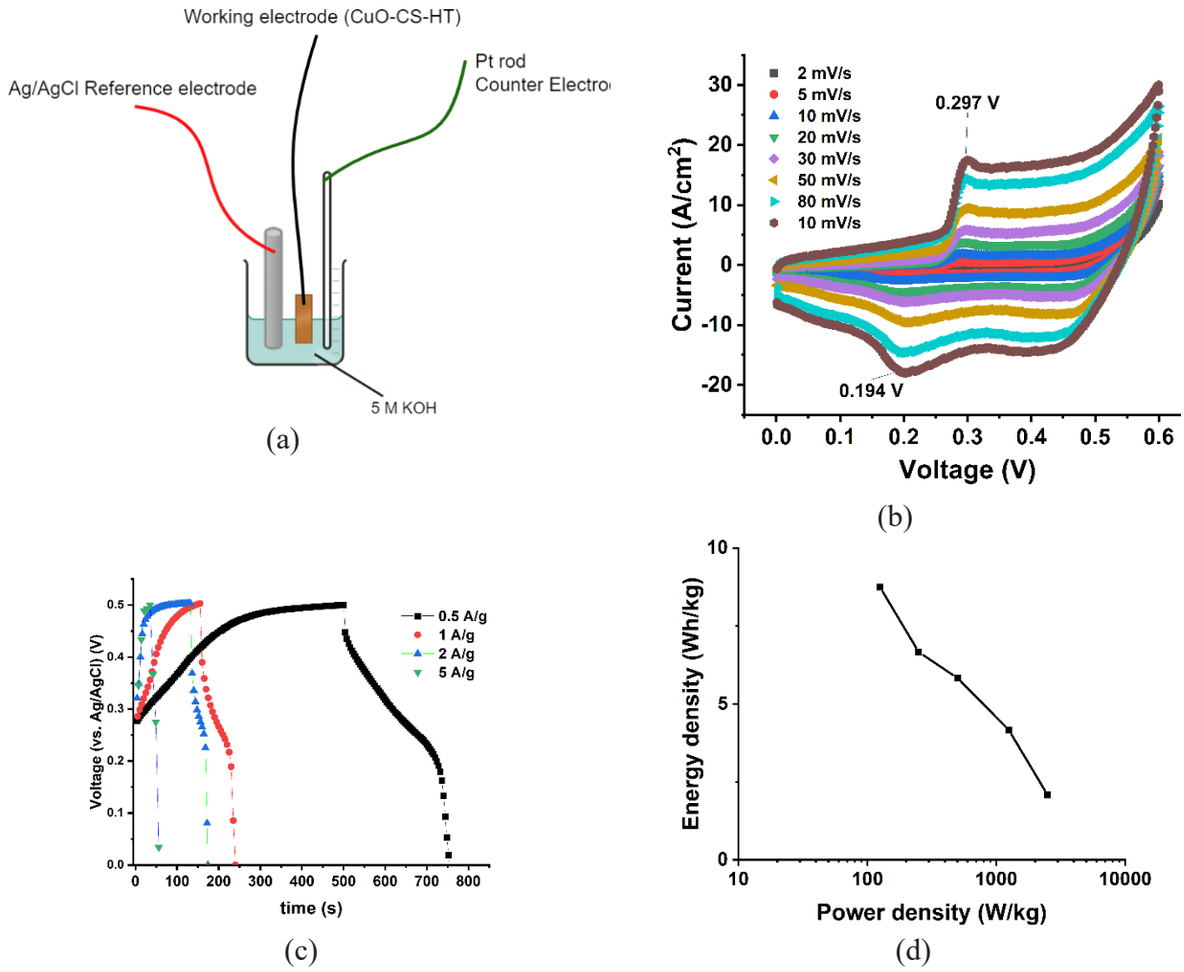

FIGURE 6. (a) The schematic diagram of electrochemical analysis using of supercapacitor using three-electrode system, (b) Cyclic Voltammogram of CuO-CS-HT at various scan-rates, (c) The GCD- Curve of CuO-CS-HT and (d) The Ragone plot of CuO-CS-HT

TABLE 3. Comparison of CuO synthesis towards their capacitance in aqueous supercapacitor

Synthesis method	Electrode	Electrolyte	Specific Capacitance	Technique	Reference
Electrodeposition of $CuSO_4$	CuO/SCE	1 M Na_2SO_4	179 F/g	Cyclic Voltammetry	Dubal et al. (2013)
Surfactant-assisted precipitation	CuO/Ag-AgCl	1 M Na_2SO_4	326 F/g	Galvanostatic Charge-Discharge	Saravanakumar et al. (2019)
Green synthesis using corn husk extract	CuO/Ag-AgCl	1 M Na_2SO_4	252 F/g	Cyclic Voltammetry	Nwanya et al. (2019)
Successive ionic layer adsorption and reaction (SILAR)	CuO/Ag-AgCl	1 M KOH	184 F/g	Cyclic Voltammetry	Patil et al. (2017)
Green synthesis using *Camellia sinensis* and copper waste	CuO/Ag-AgCl	5 M KOH	252 F/g at 0.5 A/g	Galvanostatic charge-discharge	This study

Conclusions

The biotreated lactic acid-leaching of copper wires leachate to generate Cu and CuO powders are successfully conducted as an effort to upcycle copper cable wastes. XRD, FTIR and SEM analysis confirm a monoclinic structure of CuO with a raspberry-like secondary particle with nano-sized primary particle. UV-Visible analysis of CuO confirmed the energy gap of the CuO. Based on the photocatalytic analysis, the as-prepared CuO successfully removed the presence of AO7 and MO dyes with the efficiency of more than 90%. The electrochemical performance of CuO as an active material for capacitors confirmed that the as-prepared CuO exhibited a specific capacitance of 120 F/g at a 5 A/g current rate. Overall, this economical and eco-friendly approach is highly recommended for the handling and processing of metal-containing wastes and upcycle them into multipurpose advanced metal powders.

Acknowledgments

The authors would like to express their gratitude for the research funding from Lembaga Penelitian dan Pengabdian Masyarakat Universitas Sebelas Maret (LPPM-UNS) through the HGR research grant scheme with contract number 228/UN27.22/PT.01.03/2023.

References

Addanki, S., Amiri, I.S. & Yupapin, P. 2018. Review of optical fibers-introduction and applications in fiber lasers. *Results in Physics* 10: 743-750. https://doi.org/10.1016/j.rinp.2018.07.028

Bekru, A.G., Tufa, L.T., Zelekew, O.A., Goddati, M., Lee, J. & Sabir, F.K. 2022. Green synthesis of a CuO-ZnO nanocomposite for efficient photodegradation of methylene blue and reduction of 4-Nitrophenol. *ACS Omega* 7(35): 30908-30919. https://doi.org/10.1021/acsomega.2c02687

Betim, F.S., Marins, A.A.L., Coelho, E.L.D., Lelis, M.F.F. & Freitas, M.B.J.G. 2023. Evaluation of photocatalytic properties of zinc and cobalt mixed oxide recycled from spent Li-ion and Zn–MnO_2 batteries in photo-fenton-like process. *Materials Research Bulletin* 162: 112179. https://doi.org/10.1016/j.materresbull.2023.112179

Gennero De Chialvo, M.R., Marchiano, S.L. & Arvía, A.J. 1984. The mechanism of oxidation of copper in alkaline solutions. *Journal of Applied Electrochemistry* 14(2): 165-175. https://doi.org/10.1007/BF00618735

Cuong, H.N., Pansambal, S., Ghotekar, S., Oza, R., Hai, N.T.T., Viet, N.M. & Nguyen, V.H. 2022. New frontiers in the plant extract mediated biosynthesis of copper oxide (CuO) nanoparticles and their potential applications: A review. *Environmental Research* 203: 111858. https://doi.org/10.1016/j.envres.2021.111858

Dana, A. & Sheibani, S. 2021. CNTs-copper oxide nanocomposite photocatalyst with high visible light degradation efficiency. *Advanced Powder Technology* 32(10): 3760-3769. https://doi.org/10.1016/j.apt.2021.08.023

Dharshini Perumal, Che Azurahanim Che Abdullah, Emmellie Laura Albert & Ruzniza Mohd Zawawi. 2023. Green synthesis of silver nanoparticle decorated on reduced graphene oxide nanocomposite using *Clinacanthus nutans* and its applications. *Sains Malaysiana* 52(3): 953-966. https://doi.org/10.17576/jsm-2023-5203-19

Devanthiran Letchumanan, Sophia P.M. Sok, Suriani Ibrahim, Noor Hasima Nagoor & Norhafiza Mohd Arshad. 2021. Plant-based biosynthesis of Copper/Copper Oxide nanoparticles: An update on their applications in biomedicine, mechanisms, and toxicity. *Biomolecules* 11(4): 564. https://doi.org/10.3390/biom11040564

Dong, C., Xing, M. & Zhang, J. 2020. Recent progress of photocatalytic fenton-like process for environmental remediation. *Frontiers in Environmental Chemistry* 1: 1-21. https://doi.org/10.3389/fenvc.2020.00008

Dubal, D.P., Gund, G.S., Lokhande, C.D. & Holze, R. 2013. CuO cauliflowers for supercapacitor application: Novel potentiodynamic deposition. *Materials Research Bulletin* 48(2): 923-928. https://doi.org/10.1016/j.materresbull.2012.11.081

Emima Jeronsia, J., Joseph, L.A., Vinosha, P.A., Mary, A.J. & Das, S.J. 2019. *Camellia sinensis* leaf extract mediated synthesis of copper oxide nanostructures for potential biomedical applications. *Materials Today: Proceedings* 8: 214-222. https://doi.org/10.1016/j.matpr.2019.02.103

Ghidan, A.Y., Al-Antary, T.M. & Awwad, A.M. 2016. Green synthesis of copper oxide nanoparticles using *Punica granatum* peels extract: Effect on green peach aphid. *Environmental Nanotechnology, Monitoring and Management* 6: 95-98. https://doi.org/10.1016/j.enmm.2016.08.002

Habbache, N., Alane, N., Djerad, S. & Tifouti, L. 2009. Leaching of copper oxide with different acid solutions. *Chemical Engineering Journal* 152(2-3): 503-508. https://doi.org/10.1016/j.cej.2009.05.020

Hendri Widiyandari, Orien Prilita, Muhammad Shalahuddin Al Ja'farawy, Fahru Nurosyid, Osi Arutanti, Yayuk Astuti & Nandang Mufti. 2023. Nitrogen-doped carbon quantum dots supported zinc oxide (ZnO/N-CQD) nanoflower photocatalyst for methylene blue photodegradation. *Results in Engineering* 17: 100814. https://doi.org/10.1016/j.rineng.2022.100814

Hojat Veisi, Bikash Karmakar, Taiebeh Tamoradi, Saba Hemmati, Malak Hekmati & Mona Hamelian. 2021. Biosynthesis of CuO nanoparticles using aqueous extract of herbal tea (*Stachys lavandulifolia*) flowers and evaluation of its catalytic activity. *Scientific Reports* 11: 1983. https://doi.org/10.1038/s41598-021-81320-6

Hyba, A.M., El Refay, H.M., Shahen, S. & Gaber, G.A. 2023. Comparison fabrication, identification and avoidance of corrosion potential of M-CuO NPs/S-CuO NPs to suppress corrosion on steel in an acidic solution. *Chemical Papers* 2023: 0123456789. https://doi.org/10.1007/s11696-023-02871-8

Jadhav, L.D., Patil, S.P., Chavan, A.U., Jamale, A.P. & Puri, V.R. 2011. Solution combustion synthesis of Cu nanoparticles: A role of oxidant-to-fuel ratio. *Micro and Nano Letters* 6(9): 812-815. https://doi.org/10.1049/mnl.2011.0372

Kayalvizhi, S., Sengottaiyan, A., Selvankumar, T., Senthilkumar, B., Sudhakar, C. & Selvam, K. 2020. Eco-friendly cost-effective approach for synthesis of copper oxide nanoparticles for enhanced photocatalytic performance. *Optik* 202: 163507. https://doi.org/10.1016/j.ijleo.2019.163507

Lambert, F., Gaydardzhiev, S., Léonard, G., Lewis, G., Bareel, P.F. & Bastin, D. 2015. Copper leaching from waste electric cables by biohydrometallurgy. *Minerals Engineering* 76: 38-46. https://doi.org/10.1016/J.MINENG.2014.12.029

Li, L., Bian, Y., Zhang, X., Guan, Y., Fan, E., Wu, F. & Chen, R. 2018. Process for recycling mixed-cathode materials from spent lithium-ion batteries and kinetics of leaching. *Waste Management* 71: 362-371. https://doi.org/10.1016/j.wasman.2017.10.028

Li, L., Lu, J., Ren, Y., Zhang, X.X., Chen, R.J., Wu, F. & Amine, K. 2012. Ascorbic-acid-assisted recovery of cobalt and lithium from spent Li-ion batteries. *Journal of Power Sources* 218: 21-27. https://doi.org/10.1016/j.jpowsour.2012.06.068

Lingaraju, K., Raja Naika, H., Manjunath, K., Nagaraju, G., Suresh, D. & Nagabhushana, H. 2015. Rauvolfia serpentina-mediated green synthesis of CuO nanoparticles and its multidisciplinary studies. *Acta Metallurgica Sinica (English Letters)* 28(9): 1134-1140. https://doi.org/10.1007/s40195-015-0304-y

Lisińska, M., Gajda, B., Saternus, M., Brozová, S., Wojtal, T. & Rzelewska-Piekut, M. 2022. The effect of organic acids as leaching agents for hydrometallurgical recovery of metals from PCBs. *Metalurgija* 61(3-4): 609-612.

Liu, Q., Deng, W., Wang, Q., Lin, X., Gong, L., Liu, C., Xiong, W. & Nie, X. 2020. An efficient chemical precipitation route to fabricate 3D flower-like CuO and 2D leaf-like CuO for degradation of methylene blue. *Advanced Powder Technology* 31(4): 1391-1401. https://doi.org/10.1016/j.apt.2020.01.003

Manjari, G., Saran, S., Arun, T., Vijaya Bhaskara Rao, A. & Devipriya, S.P. 2017. Catalytic and recyclability properties of phytogenic copper oxide nanoparticles derived from *Aglaia elaeagnoidea* flower extract. *Journal of Saudi Chemical Society* 21(5): 610-618. https://doi.org/10.1016/j.jscs.2017.02.004

Meghana Navada, K., Nagaraja, G.K., D'Souza, J.N., Kouser, S., Ranjitha, R. & Manasa, D.J. 2020. Phyto assisted synthesis and characterization of *Scoparia dulsis* L. leaf extract mediated porous nano CuO photocatalysts and its anticancer behavior. *Applied Nanoscience (Switzerland)* 10(11): 4221-4240. https://doi.org/10.1007/s13204-020-01536-2

Muhammad Aadil, Abdur Rahman, Sonia Zulfiqar, Ibrahim A. Alsafari, Muhammad Shahid, Imran Shakir, Philips O. Agboola, Sajjad Haider & Muhammad Farooq Warsi. 2021. Facile synthesis of binary metal substituted copper oxide as a solar light driven photocatalyst and antibacterial substitute. *Advanced Powder Technology* 32(3): 940-950. https://doi.org/10.1016/j.apt.2021.01.040

Nagaraj, E., Karuppannan, K., Shanmugam, P. & Venugopal, S. 2019. Exploration of bio-synthesized copper oxide nanoparticles using *Pterolobium hexapetalum* leaf extract by photocatalytic activity and biological evaluations. *Journal of Cluster Science* 30(4): 1157-1168. https://doi.org/10.1007/s10876-019-01579-8

Nagarajan, N. & Panchatcharam, P. 2023. Cost-effective and eco-friendly copper recovery from waste printed circuit boards using organic chemical leaching. *Heliyon* 9(3): e13806. https://doi.org/10.1016/j.heliyon.2023.e13806

Nisha, B., Vidyalakshmi, Y. & Sirajunnisa Abdul Razack. 2020. Enhanced formation of ruthenium oxide nanoparticles through green synthesis for highly efficient supercapacitor applications. *Advanced Powder Technology* 31(3): 1001-1006. https://doi.org/10.1016/j.apt.2019.12.026

Nwanya, A.C., Ndipingwi, M.M., Mayedwaa, N., Razanamahandry, L.C., Ikpo, C.O., Waryo, T., Ntwampe, S.K.O., Malenga, E., Fosso-Kankeu, E., Ezema, F.I., Iwuoha, E.I. & Maaza, M. 2019. Maize (*Zea mays* L.) fresh husk mediated biosynthesis of copper oxides: Potentials for pseudo capacitive energy storage. *Electrochimica Acta* 301: 436-448. https://doi.org/10.1016/j.electacta.2019.01.186

Pakzad, K., Alinezhad, H. & Nasrollahzadeh, M. 2019. Green synthesis of Ni@Fe3O4 and CuO nanoparticles using *Euphorbia maculata* extract as photocatalysts for the degradation of organic pollutants under UV-irradiation. *Ceramics International* 45(14): 17173-17182. https://doi.org/10.1016/j.ceramint.2019.05.272

Patil, A.S., Patil, M.D., Lohar, G.M., Jadhav, S.T. & Fulari, V.J. 2017. Supercapacitive properties of CuO thin films using modified SILAR method. *Ionics* 23(5): 1259-1266. https://doi.org/10.1007/s11581-016-1921-9

Qaderi, J., Mamat, C.R. & Abdul Jalil, A. 2021. "Preparation and Characterization of Copper, Iron, and Nickel Doped Titanium Dioxide Photocatalysts for Decolorization of Methylene Blue." *Sains Malaysiana* 50 (1): 135–49. https://doi.org/10.17576/jsm-2021-5001-14.

Raub, Aini Ayunni Mohd, Jumril Yunas, Mohd Ambri Mohamed, Jamal Kazmi, Jaenudin Ridwan, and Azrul Azlan Hamzah. 2022. "Statistical Optimization of Zinc Oxide Nanorod Synthesis for Photocatalytic Degradation of Methylene Blue." *Sains Malaysiana* 51 (6): 1933–44. https://doi.org/10.17576/jsm-2022-5106-28.

Rostami-Vartooni, Akbar. 2017. "Green Synthesis of CuO Nanoparticles Loaded on the Seashell Surface Using Rumex Crispus Seeds Extract and Its Catalytic Applications for Reduction of Dyes." *IET Nanobiotechnology* 11 (4): 349–59. https://doi.org/10.1049/iet-nbt.2016.0149.

Saquf Jillani, Mohsan Jelani, Najam Ul Hassan, Shahbaz Ahmad & Muhammad Hafeez. 2018. Synthesis, characterization and biological studies of copper oxide nanostructures. *Materials Research Express* 5(4). https://doi.org/10.1088/2053-1591/aab864

Saravanakumar, Balakrishnan, Chandran Radhakrishnan, Murugan Ramasamy, Rajendran Kaliaperumal, Allen J. Britten, and Martin Mkandawire. 2019. "Surfactant Determines the Morphology, Structure and Energy Storage Features of CuO Nanostructures." *Results in Physics* 13 (March): 102185. https://doi.org/10.1016/j.rinp.2019.102185.

Seong, Won Mo & Manthiram, A. 2020. "Complementary Effects of Mg and Cu Incorporation in Stabilizing the Cobalt-Free $LiNiO_2$Cathode for Lithium-Ion Batteries." *ACS Applied Materials and Interfaces* 12 (39): 43653–64. https://doi.org/10.1021/acsami.0c11413.

Shah, Rosmahani Mohd, Rozan Mohamad Yunus, Mohd Shahbudin Masdar Mastar, Lorna Jefferey Minggu, Wai Yin Wong, and Abdul Amir H. Kadhum. 2019. "Synthesis of Graphene/Cu2O Thin Film Photoelectrode via Facile Hydrothermal Method for Photoelectrochemical Measurement." *Sains Malaysiana* 48 (6): 1233–38. https://doi.org/10.17576/jsm-2019-4806-10.

Shanmugam Prakash, Nagaraj Elavarasan, Alagesan Venkatesan, Kasivisvanathan Subashini, Murugesan Sowndharya & Venugopal Sujatha. 2018. Green synthesis of copper oxide nanoparticles and its effective applications in Biginelli reaction, BTB photodegradation and antibacterial activity. *Advanced Powder Technology* 29(12): 3315-3326. https://doi.org/10.1016/j.apt.2018.09.009

Soraya Ulfa Muzayanha, Cornelius Satria Yudha, Adrian Nur, Hendri Widiyandari, Hery Haerudin, Hanida Nilasary, Ferry Fathoni & Agus Purwanto. 2019. A fast metals recovery method for the synthesis of lithium nickel cobalt aluminum oxide material from cathode waste. *Metals* 9(5): 615. https://doi.org/10.3390/met9050615

Tanna, J.A., Chaudhary, R.G., Gandhare, N.V., Rai, A.R., Yerpude, S. & Juneja, H.D. 2016. Copper nanoparticles catalysed an efficient one-pot multicomponents synthesis of chromenes derivatives and its antibacterial activity. *Journal of Experimental Nanoscience* 11(11): 884-900. https://doi.org/10.1080/17458080.2016.1177216

Varughese, A., Kaur, R. & Singh, P. 2020. Green synthesis and characterization of copper oxide nanoparticles using *Psidium guajava* leaf extract. *IOP Conference Series: Materials Science and Engineering* 961: 012011. https://doi.org/10.1088/1757-899X/961/1/012011

Zhuang, L., Sun, C., Zhou, T., Li, H. & Dai, A. 2019. Recovery of valuable metals from $LiNi_{0.5}Co_{0.2}Mn_{0.3}O_2$ cathode materials of spent Li-ion batteries using mild mixed acid as leachant. *Waste Management* 85: 175-185. https://doi.org/10.1016/j.wasman.2018.12.034

*Corresponding author; email: corneliussyudha@staff.uns.ac.id